20

Outlook: dynamics in plastic networks

In this final chapter, we combine the dynamics of single neurons (Parts I and II) and networks (Part III) with synaptic plasticity (Chapter 19) and illustrate their interaction in a few applications.

In Section 20.1 on "reservoir computing" we show that the network dynamics in random networks of excitatory and inhibitory neurons is sufficiently rich to serve as a computing device that buffers past inputs and computes on present ones. In Section 20.2 we study oscillations that arise in networks of spiking neurons and outline how synaptic plasticity interacts with oscillations. Finally, in Section 20.3, we illustrate why the study of neuronal dynamics is not just an intellectual exercise, but might, one day, become useful for applications or, eventually, benefit human patients.

20.1 Reservoir computing

One of the reasons the dynamics of neuronal networks are rich is that networks have a nontrivial connectivity structure linking different neuron types in an intricate interaction pattern. Moreover, network dynamics are rich because they span many time scales. The fastest time scale is set by the duration of an action potential, i.e., a few milliseconds. Synaptic facilitation and depression (Chapter 3) or adaptation (Chapter 6) occur on time scales from a few hundred milliseconds to seconds. Finally, long-lasting changes of synapses can be induced in a few seconds, but last from hours to days (Chapter 19).

These rich dynamics of neuronal networks can be used as a "reservoir" for intermediate storage and representation of incoming input signals. Desired outputs can then be constructed by reading out appropriate combinations of neuronal spike trains from the network. This kind of "reservoir computing" encompasses the notions of "liquid computing" (Maass *et al*., 2002) and "echo state networks" (Jaeger and Haas, 2004). Before we discuss some mathematical aspects of randomly connected networks, we illustrate rich dynamics by a simulated model network.

https://doi.org/10.1017/CBO9781107447615.024 Published online by Cambridge University Press

20.1.1 Rich dynamics

A nice example of rich network dynamics is the work by Maass *et al*. (2007). Six hundred leaky integrate-and-fire neurons (80 % excitatory and 20 % inhibitory) were placed on a three-dimensional grid with distance-dependent random connectivity of small probability so that the total number of synapses is about 10 000. Synaptic dynamics included short-term plasticity (Chapter 3) with time constants ranging from a few tens of milliseconds to a few seconds. Neuronal parameters varied from one neuron to the next and each neuron received independent noise.

To check the computational capabilities of such a network, Maass *et al*. stimulated it with four input streams targeting different subgroups of the network (Fig. 20.1). Each input stream consisted of Poisson spike trains with time-dependent firing rate $\nu(t)$.

Streams 1 and 2 fired at a low background rate but switched occasionally to a short period of high firing rate ("burst"). In order to build a memory of past bursts, synaptic weights from the network onto a group of eight integrate-and-fire neurons ("memory" in Fig. 20.1) were adjusted by an optimization algorithm, so that the spiking activity of these eight neurons reflects whether the last firing rate burst happened in stream 1 (memory neurons are active = memory "on") or 2 (the same neurons are inactive = memory "off"). Thus, these neurons provided a 1-bit memory ("on"/"off") of past events.

Streams 3 and 4 were used to perform a non-trivial online computation. A network output with value ν_{online} was optimized to calculate the sum of activity in streams 3 and 4, but only if the memory neurons were active (memory "on"). Optimization of weight parameters was achieved in a series of preliminary training trials by minimizing the squared error (Chapter 10) between the target and the actual output.

Figure 20.1 shows that, after optimization of the weights, the network could store a memory and, at the same time, perform the desired online computation. Therefore, the dynamics in a randomly connected network with feedback from the output are rich enough to generate an output stream which is a non-trivial nonlinear transformation of the input streams (Maass *et al*., 2007; Jaeger and Haas, 2004; Sussillo and Abbott, 2009).

In the above simulation, the tunable connections (Fig. 20.1a) have been adjusted "by hand" (or rather by a suitable algorithm), in a biologically non-plausible fashion, so as to yield the desired output. However, it is possible to learn the desired output with the three-factor learning rules discussed in Section 19.4. This has been demonstrated on a task and set-up very similar to Fig. 20.1, except that the neurons in the network were modeled by rate units (Hoerzer *et al*., 2012). The neuromodulatory signal M (see Section 19.4) took a value of 1 if the momentary performance was better than the average performance in the recent past, and zero otherwise.

20.1.2 Network analysis (*)

Networks of randomly connected excitatory and inhibitory neurons can be analyzed for the case of rate units (Rajan and Abbott, 2006). Let x_i denote the deviation from a spontaneous

https://doi.org/10.1017/CBO9781107447615.024 Published online by Cambridge University Press

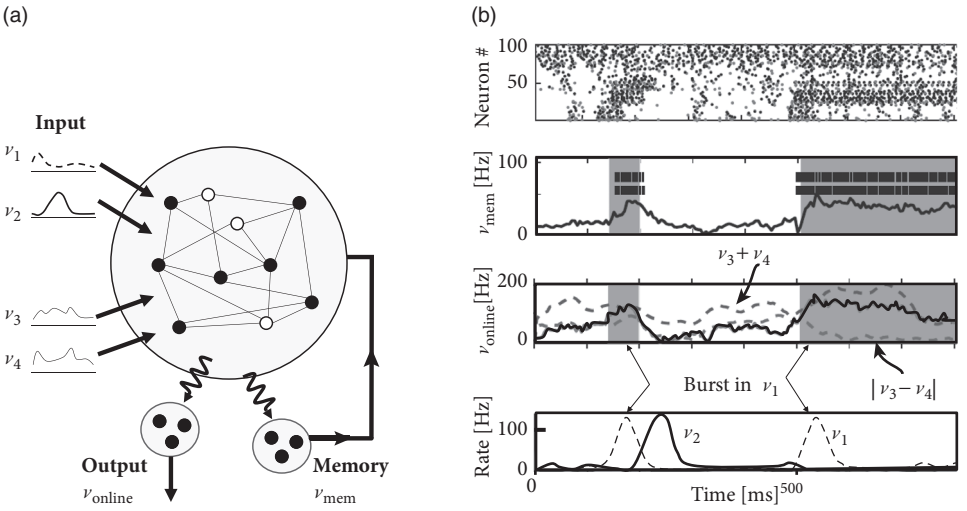

Fig. 20.1 Reservoir computing. (a) A randomly connected network of integrate-and-fire neurons receives four input streams, each characterized by spike trains with a time-dependent Poisson firing rate ν_k. The main network is connected to two further pools of neurons, called "memory" and "output." Memory neurons are trained to fire at high rates if the last burst in ν_1 is more recent than the last burst in ν_2. Spike trains of the memory neurons are fed back into the network. The output ν_{online} is trained to calculate either the sum $\nu_3 + \nu_4$ or the difference $|\nu_3 - \nu_4|$ of the two other input streams, depending on the current setting of the memory unit. The tunable connections onto the memory and output neurons are indicated by curly arrows. (b) Spiking activity of the main network (top) and of two memory neurons (second from top) as well as mean firing rate of memory neurons (second from top), and online output (third, thick solid line; the dashed lines give the momentary targets). The two input streams ν_1, ν_2 are shown at the bottom. The periods when the memory unit should be active are shaded. Adapted from Maass *et al*. (2007).

background rate ν_0, i.e., the rate of neuron i is $\nu_i = \nu_0 + x_i$. Let us consider the update dynamics

$$x_i(t+1) = g\left(\sum_j w_{ij} x_j\right) \tag{20.1}$$

for a monotone transfer function g with $g(0) = 0$ and derivative $g'(0) = 1$.

The background state ($x_i = 0$ for all neurons i) is stable if the weight matrix has no eigenvalues with real part larger than 1. If there are eigenvalues with real part larger than 1, spontaneous chaotic network activity may occur (Sompolinksy *et al*., 1988).

For weight matrices of random networks, a surprising number of mathematical results exist. We focus on mixed networks of excitatory and inhibitory neurons. In a network of N neurons, there are fN excitatory and $(1-f)N$ inhibitory neurons where f is the fraction of excitatory neurons. Outgoing weights from an excitatory neuron j take values $w_{ij} \geq 0$ for all i (and $w_{ij} \leq 0$ for weights from inhibitory neurons), so that all columns

https://doi.org/10.1017/CBO9781107447615.024 Published online by Cambridge University Press

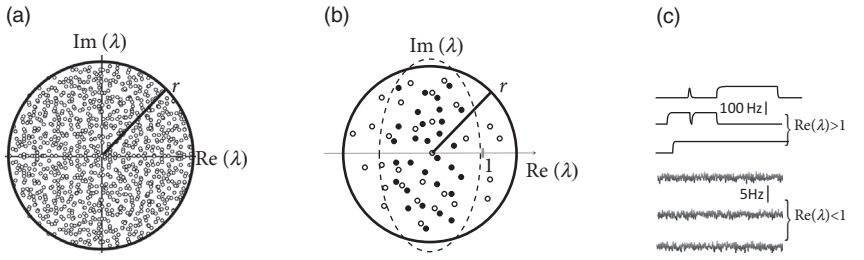

Fig. 20.2 Random networks. (a) Distribution of eigenvalues in the complex plane for a network of excitatory and inhibitory neurons with detailed balance. The distribution is circular and stays within a spectral radius r. Adapted from Rajan and Abbott (2006). (b) Inhibitory plasticity quenches the real part of eigenvalues into a smaller band (dashed ellipse). Thus an unstable random network (where some eigenvalues have $\mathrm{Re}(\lambda) > 1$, open circles) can be turned into stable one ($\mathrm{Re}(\lambda) < 1$, solid circles); schematic figure. (c) Time course of the activity of three sample neurons while the network is driven with a small amount of noise. Neuronal activity in unstable random networks exhibits chaotic switching between maximally low and high rates (top three traces) whereas the same neurons show only a small amount of fluctuations after stabilization through inhibitory plasticity (bottom three traces). Adapted from Hennequin (2014).

of the weight matrix have the same sign. We assume non-plastic random weights with the following three constraints: (i) Input to each neuron is balanced so that $\sum_j w_{ij} = 0$ for all i ("detailed balance"). In other words, if all neurons are equally active, excitation and inhibition cancel each other on a neuron-by-neuron level. (ii) Excitatory weights are drawn from a distribution with mean $\mu_\mathrm{E}/\sqrt{N} > 0$ and variance r/N. (iii) Inhibitory weights are drawn from a distribution with mean $\mu_\mathrm{I}/\sqrt{N} < 0$ and variance r/N. Under the conditions (i)–(iii), the eigenvalues of the weight matrix all lie within a circle (Fig. 20.2a) of radius r, called the spectral radius (Rajan and Abbott, 2006).

The condition of detailed balance stated above as item (i) may look artificial at first sight. However, experimental data supports the idea of detailed balance (Froemke *et al.*, 2007; Okun and Lampl, 2008). Moreover, plasticity of inhibitory synapses can be used to achieve such a balance of excitation and inhibition on a neuron-by-neuron basis (Vogels *et al.*, 2011).

To understand how inhibitory plasticity comes into play, consider a rate model in continuous time

$$\tau \frac{\mathrm{d}x_i}{\mathrm{d}t} = -x_i + g\left(\sum_j w_{ij} x_j\right) + \xi(t), \tag{20.2}$$

where τ is a time constant and x_i is, as before, the deviation of the firing rate from a background level ν_0. The gain function $g(h)$ with $g(0)$ and $g'(0) = 1$ is bounded between $x^{\min} = -\nu_0$ and $x^{\max}$. Gaussian white noise $\xi(t)$ of small amplitude is added on the right-hand side of Eq. (20.2) to kick network activity out of the fixed point at $x = 0$.

We subject inhibitory weights $w_{ij} < 0$ (where j is one of the inhibitory neurons) to

https://doi.org/10.1017/CBO9781107447615.024 Published online by Cambridge University Press

Hebbian plasticity

$$\frac{\mathrm{d}}{\mathrm{d}t} w_{ij} = -\gamma x_i(t)\bar{x}_j(t), \tag{20.3}$$

where $\bar{x}_j(t) = \int_0^\infty \exp(-s/\tau)\, x_j(t-s)\mathrm{d}s$ is the synaptic trace left by earlier presynaptic activity. For $\gamma > 0$, this is a Hebbian learning rule because the absolute size of the *inhibitory* weight increases if postsynaptic and presynaptic activity are correlated (Chapter 19).

In a random network of $N = 200$ excitatory and inhibitory rate neurons with an initial weight matrix that had a large distribution of eigenvalues, inhibitory plasticity according to Eq. (20.3) led to a compression of the real parts of the eigenvalues (Hennequin, 2013). Hebbian inhibitory plasticity can therefore push a network from the regime of unstable dynamics into a stable regime (Fig. 20.2b,c) while keeping the excitatory weights strong. Such networks, which have strong excitatory connections, counterbalanced by equally strong precisely tuned inhibition, can potentially explain patterns of neural activity in the motor cortex during arm movements (Churchland *et al*., 2012). In-depth understanding of patterns in the motor cortex could eventually contribute to the development of neural prosthesis (Shenoy *et al*., 2011) that detect and decode neural activity in motor-related brain areas and translate it into intended movements of a prosthetic limb; see Chapter 11.

Example: Generating movement trajectories with inhibition stabilized networks

During the preparation and performance of arm movements (Fig. 20.3a) neurons in the motor cortex exhibit collective dynamics (Churchland *et al*., 2012). In particular, during the preparation phase just before the start of the movement, the network activity approaches a stable pattern of firing rates, which is similar across different trials. This stable pattern can be interpreted as an initial condition for the subsequent evolution of the network dynamics during arm movement, which is rather stereotypical across trials (Shenoy *et al*., 2011).

Because of its sensitivity to small perturbations, a random network with chaotic network dynamics may not be a plausible candidate for stereotypical dynamics, necessary for reliable arm movements. On the other hand, in a stable random network with a circular distribution of eigenvalues with spectral radius $r < 1$, transient dynamics after release from an initial condition are short and dominated by the time constant τ of the single-neuron dynamics (unless one of the eigenvalues is hand-tuned to lie very close to unity). Moreover, as discussed in Chapter 18, the cortex is likely to work in the regime of an inhibition-stabilized network (Tsodyks *et al*., 1997; Ozeki *et al*., 2009) where excitatory connections are strong, but counterbalanced by even stronger inhibition.

Inhibitory plasticity is helpful to generate inhibition-stabilized random networks. Because excitatory connections are strong but random, transient activity after release from an appropriate initial condition is several times longer than the single-neuron time constant τ. Different initial conditions put the network onto different, but reliable trajectories. These trajectories of the collective network dynamics can be used as a reservoir to generate simulated muscle output for different arm trajectories (Fig. 20.3).

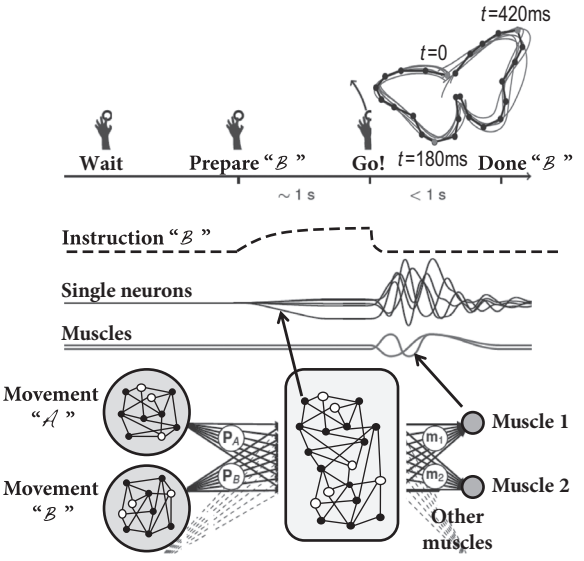

Fig. 20.3 Movement preparation and execution. Top: A typical delayed movement generation task in behavioral neuroscience starts with the instruction of what movement must be prepared. The arm must be held still until the go cue is given. Middle: During the preparatory period, model neurons receive a ramp input (dashed) which is withdrawn when the go cue is given. Thereafter the network dynamics move freely from the initial condition set during the preparatory period. Model neurons (four sample black lines) then exhibit transient oscillations which drive muscle activation (gray lines). Bottom: To prepare the movement $\mathscr{B}$ (e.g., butterfly movement), the network (gray box, middle) is initialized in the desired state by the slow activation of the corresponding pool of neurons (gray circle). Muscles (right) in the model are activated by a suitable combination of neuronal activity read out from the main network. Note that no feedback is given during the drawing movement. Adapted from Hennequin *et al*. (2014).

20.2 Oscillations: good or bad?

Oscillations are a prevalent phenomenon in biological neural systems and manifest themselves experimentally in electroencephalograms (EEG), recordings of local field potentials (LFP), and multi-unit recordings. Oscillations are thought to stem from synchronous network activity and are often characterized by the associated frequency peak in the Fourier spectrum. For example, oscillations in the range 30–70 Hz are called gamma oscillations and those above 100 Hz "ultrafast" or "ripples" (Traub, 2006; Buzsaki, 2011). Among the slower oscillations, prominent examples are delta oscillations (1–4 Hz) and spindle oscillations in the EEG during sleep (7–15 Hz) (Bazhenov and Timofeev, 2006) or theta oscillations (4–10 Hz) in the hippocampus and other areas (Buzsaki, 2011).

Oscillations are thought to play an important role in the coding of sensory information. In the olfactory system an ongoing oscillation of the population activity provides a temporal frame of reference for neurons coding information about the odorant (Laurent, 1996).

https://doi.org/10.1017/CBO9781107447615.024 Published online by Cambridge University Press

Similarly, place cells in the hippocampus exhibit phase-dependent firing activity relative to a background oscillation (O'Keefe and Recce, 1993; Buzsaki, 2011). Moreover, rhythmic spike patterns in the inferior olive may be involved in various timing tasks and motor coordination (Welsh *et al*., 1995; Kistler and van Hemmen, 2000). Finally, synchronization of firing across groups of neurons has been hypothesized to provide a potential solution to the so-called binding problem (Singer, 1993, 2007). The common idea across all the above examples is that an oscillation provides a reference signal for a "phase code": the significance of a spike depends on its phase with respect to the global oscillatory reference; see Section 7.6 and Fig. 7.17. Thus, oscillations are potentially useful for intricate neural coding schemes.

On the other hand, synchronous oscillatory brain activity is correlated with numerous brain diseases. For example, an epileptic seizure is defined as "a transient occurrence of signs and/or symptoms due to abnormal excessive or synchronous neuronal activity in the brain" (Fisher *et al*., 2005). Similarly, Parkinson's disease is characterized by a high level of neuronal synchrony in the thalamus and basal ganglia (Pare *et al*., 1990) while neurons in the same areas fire asynchronously in the healthy brain (Nini *et al*., 1995). Moreover, local field potential oscillations at theta frequency in thalamic or subthalamic nuclei are linked to tremor in human Parkinsonian patients, i.e., rhythmic finger, hand or arm movement at 3–6 Hz (Pare *et al*., 1990; Tass *et al*., 2010). Therefore, in these and in similar situations, it seems to be desirable to suppress abnormal, highly synchronous oscillations so as to shift the brain back into its healthy state.

Simulations of the population activity in homogeneous networks typically exhibit oscillations when driven by a constant external input. For example, oscillations in networks of purely excitatory neurons arise because, as soon as some neurons in the network fire, they contribute to exciting others. Once the avalanche of firing has run across the network, all neurons pass through a period of refractoriness, until they are ready to fire again. In this case the time scale of the oscillation is set by neuronal refractoriness (Fig. 20.4a). A similar argument can be made for a homogeneous network of inhibitory neurons driven by a constant external stimulus. After a first burst by a few neurons, mutual inhibition will silence the population until inhibition wears off. Thereafter, the whole network fires again.

Oscillations also arise in networks of coupled excitatory and inhibitory neurons. The excitatory connections cause a synchronous bursts of the network activity leading to a build-up of inhibition which, in turn, suppresses the activity of excitatory neurons. The oscillation period in the two latter cases is therefore set by the build-up and decay time of inhibitory feedback (Fig. 20.4b).

Even slower oscillations can be generated in "winner-take-all" networks (see Chapter 16) with dynamic synapses (see Chapter 3) or adaptation (see Chapter 6). Suppose the networks consists of K populations of excitatory neurons which share a common pool of inhibitory neurons. Parameters can be set such that excitatory neurons within the momentarily "winning" population stimulate each other so as to overcome inhibition. In the presence of synaptic depression, however, the mutual excitation fades away after a short time, so that now a different excitatory population becomes the new "winner" and switches on.

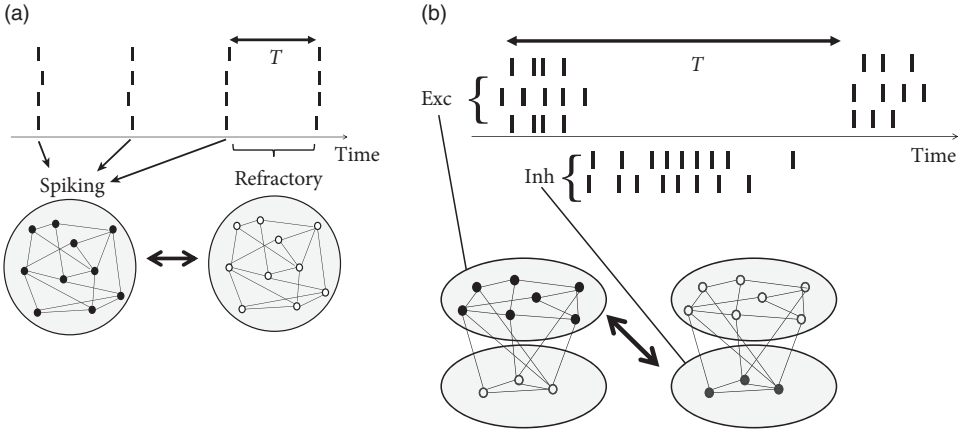

Fig. 20.4 Types of network oscillation. (a) In a homogeneous network of excitatory neurons, near-synchronous firing of all neurons is followed by a period of refractoriness, leading to fast oscillations with period T. Active neurons: vertical dash in spike raster and solid circle in network schema. Silent neurons: open circle in schema. (b) In a network of excitatory and inhibitory neurons, activity of the excitatory population alternates with activity of the inhibitory one. The period T is longer than in (a).

As a result, inhibition arising from inhibitory neurons turns the activity of the previously winning group off, until inhibition has decayed and excitatory synapses have recovered from depression. The time scale is then set by a combination of the time scales of inhibition and synaptic depression. Networks of this type have been used to explain the shift of attention from one point in a visual scene to the next (Itti *et al*., 1998).

In this section, we briefly review mathematical theories of oscillatory activity (Sections 20.2.1–20.2.3) before we study the interaction of oscillations with STDP (Section 20.2.4) The results of this section will form the basis for the discussion of Section 20.3.

20.2.1 Synchronous oscillations and locking

Homogeneous networks of spiking neurons show a natural tendency toward oscillatory activity. In Sections 13.4.2 and 14.2.3, we analyzed the stability of asynchronous firing. In the stationary state the population activity is characterized by a constant value A_0 of the population activity. An instability of the dynamics with respect to oscillations at period T, appears as a sinusoidal perturbation of increasing amplitude; see Fig. 20.5a as well as Fig. 14.8. The analysis of the stationary state shows that a high level of noise, network heterogeneity, or a sufficient amount of inhibitory plasticity, all contribute to stabilizing the stationary state. The linear stability analysis, however, is only valid in the vicinity of the stationary state. As soon as the amplitude ΔA of the oscillations is of the same order of magnitude as A_0, the solution found by linear analysis is no longer valid since the population activity cannot become negative.

Oscillations can, however, also be analyzed from a completely different perspective. In a homogeneous network with fixed connectivity in the limit of low noise we expect strong

https://doi.org/10.1017/CBO9781107447615.024 Published online by Cambridge University Press

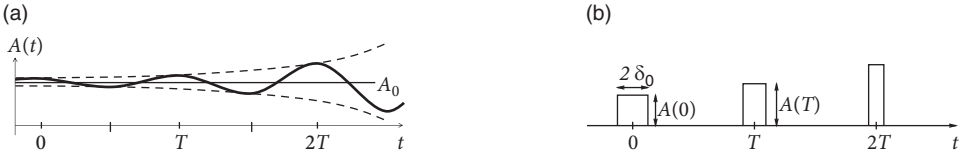

Fig. 20.5 Population activity $A(t)$ during oscillations and synchrony. (a) An instability of asynchronous firing at rate A_0 leads to a sinusoidal oscillation of increasing amplitude. (b) If the fully synchronized state is stable, the width δ_0 of the rectangular population pulses decreases while their amplitude $A(kT)$ increases with each period.

oscillations. In the following, we focus on the synchronous oscillatory mode where nearly all neurons fire in "lockstep" (Fig. 20.5b). We study whether such periodic synchronous bursts of the population activity can be a stable solution of network equations.

To keep the arguments simple, we consider a homogeneous population of identical SRM_0 neurons (Chapter 6 and Section 9.3) which is nearly perfectly synchronized and fires almost regularly with period T. To analyze the existence and stability of a fully locked synchronous oscillation we approximate the population activity by a sequence of square pulses k, $k \in \{0, \pm 1, \pm 2, \ldots\}$, centered around $t = kT$. Each pulse k has a certain half-width δ_k and amplitude $(2\delta_k)^{-1}$ – since all neurons are supposed to fire once in each pulse; see Fig. 20.5b. If we find that the amplitude of subsequent pulses increases while their width decreases (i.e., $\lim_{k\to\infty} \delta_k = 0$), we conclude that the fully locked state in which all neurons fire simultaneously is stable.

In the examples below, we will prove that the condition for stable locking of all neurons in the population can be stated as a condition on the *slope* h' of the input potential h at the moment of firing. More precisely, if the last population pulse occurred at about $t = 0$ with amplitude $A(0)$ the amplitude of the population pulse at $t = T$ increases if $h'(T) > 0$:

$$h'(T) > 0 \quad \Longleftrightarrow \quad A(T) > A(0)\,. \tag{20.4}$$

If the amplitude of subsequent pulses increases, their width must decrease accordingly. In other words, we have the following *locking theorem*. In a homogeneous network of SRM_0 neurons, a necessary and, in the limit of a large number of presynaptic neurons ($N \to \infty$), also sufficient condition for a coherent oscillation to be asymptotically stable is that firing occurs when the postsynaptic potential arising from all previous spikes in the population is increasing in time (Gerstner *et al.*, 1996b).

Example: Perfect synchrony in network of inhibitory neurons

Locking in a population of spiking neurons can be understood by simple geometrical arguments. To illustrate this argument, we study a homogeneous network of N identical SRM_0 neurons which are mutually coupled with strength $w_{ij} = J_0/N$. In other words, the interaction is scaled with $1/N$ so that the total input to a neuron i is of order 1 even if the

https://doi.org/10.1017/CBO9781107447615.024 Published online by Cambridge University Press

number of neurons is large ($N \to \infty$). Since we are interested in synchrony we suppose that all neurons have fired simultaneously at $\hat{t} = 0$. When will the neurons fire again?

Since all neurons are identical we expect that the next firing time will also be synchronous. Let us calculate the period T between one synchronous pulse and the next. We start from the firing condition of SRM_0 neurons

$$\vartheta = u_i(t) = \eta(t - \hat{t}_i) + \sum_j w_{ij} \sum_f \varepsilon\left(t - t_j^f\right) + h_0\,, \tag{20.5}$$

where $\varepsilon(t)$ is the postsynaptic potential. The axonal transmission delay Δ^{ax} is included in the definition of ε, i.e., $\varepsilon(t) = 0$ for $t < \Delta^{\mathrm{ax}}$. Since all neurons have fired synchronously at $t = 0$, we set $\hat{t}_i = t_j^f = 0$. The result is a condition of the form

$$\vartheta - \eta(t) = J_0\,\varepsilon(t) + h_0, \tag{20.6}$$

since $w_{ij} = J_0/N$ for $j = 1, \ldots, N$. Note that we have neglected the postsynaptic potentials that may have been caused by earlier spikes $t_j^f < 0$ back in the past.

The graphical solution of Eq. (20.6) for the case of inhibitory neurons (i.e., $J_0 < 0$) is presented in Fig. 20.6. The first crossing point of the effective dynamic threshold $\vartheta - \eta(t)$ and $J_0\,\varepsilon(t) + h_0$ defines the time T of the next synchronous pulse.

What happens if synchrony at $t = 0$ was not perfect? Let us assume that one of the neurons is slightly late compared to the others (Fig. 20.6b). It will receive the input $J_0\,\varepsilon(t)$ from the others, thus the right-hand side of Eq. (20.6) remains the same. The left-hand side, however, is different since the last firing was at δ_0 instead of zero. The next firing time is at $t = T + \delta_1$ where δ_1 is found from

$$\vartheta - \eta(T + \delta_1 - \delta_0) = h_0 + J_0\,\varepsilon(T + \delta_1)\,. \tag{20.7}$$

Linearization with respect to δ_0 and δ_1 then yields:

$$\delta_1 < \delta_0 \quad \Longleftrightarrow \quad J_0 \varepsilon'(T) > 0\,, \tag{20.8}$$

where we have exploited that neurons with "normal" refractoriness and adaptation properties have $\eta' > 0$. From Eq. (20.8) we conclude that the neuron which has been late is "pulled back" into the synchronized pulse of the others if the postsynaptic potential $J_0\varepsilon$ is rising at the moment of firing at T. Equation (20.8) is a special case of the locking theorem.

Example: Proof of the locking theorem (*)

To check whether the fully synchronized state is a stable solution of the network dynamics, we exploit the population integral equation (14.5) and assume that the population has already fired a couple of narrow pulses for $t < 0$ with widths $\delta_k \ll T$, $k \leq 0$, and calculate the amplitude and width of subsequent pulses.

https://doi.org/10.1017/CBO9781107447615.024 Published online by Cambridge University Press

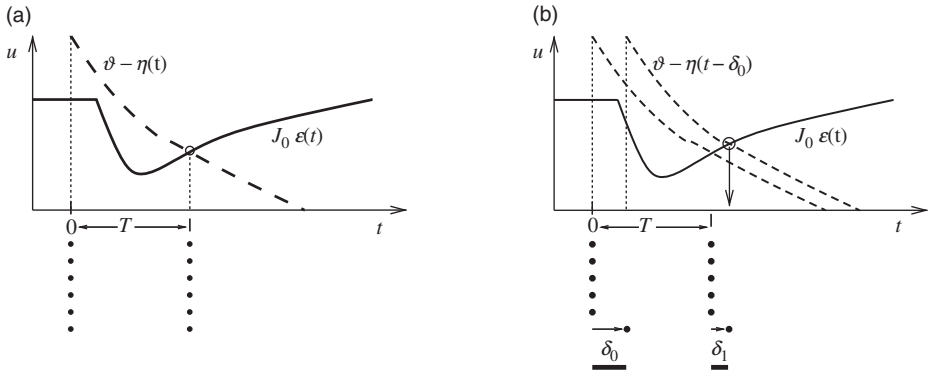

Fig. 20.6 Synchronous firing in a network with inhibitory coupling. (a) Bottom: Spike raster – all neurons have fired synchronously at $\hat{t} = 0$. Top: The next spike occurs when the total input potential $h_0 + J_0\,\varepsilon(t)$ (solid line; the offset corresponds to a constant background input $h_0 > 0$) has increased sufficiently to cross the dynamic threshold $\vartheta - \eta(t)$. (b) Stability of perfect synchrony. The last neuron is out of tune. The firing time difference at $t = 0$ is δ_0. One period later the firing time difference is reduced ($\delta_1 < \delta_0$), since the threshold is reached at a point where $J_0\,\varepsilon(t)$ is rising. Therefore this neuron is eventually pulled back into the synchronous group.

To translate the above idea into a step-by-step demonstration, we use

$$A(t) = \sum_{k=-\infty}^{\infty} \frac{1}{2\delta_k} \Theta[t - (kT - \delta_k)]\,\Theta[(kT + \delta_k) - t] \tag{20.9}$$

as a parameterization of the population activity; see Fig. 20.5b. Here, $\Theta(.)$ denotes the Heaviside step function with $\Theta(s) = 1$ for $s > 0$ and $\Theta(s) = 0$ for $s \leq 0$. For stability, we need to show that the amplitude $A(0), A(T), A(2T), \ldots$ of the rectangular pulses increases while the width δ_k of subsequent pulses decreases.

To prove the theorem, we assume that (i) all neurons in the network have identical refractoriness $\eta(s)$ with $\mathrm{d}\eta/\mathrm{d}s > 0$ for all $s > 0$; (ii) all neurons have identical shape $\varepsilon(s)$ of the postsynaptic potential; (iii) all couplings are identical, $w_{ij} = w_0 = J_0/N$; and (iv) all neurons receive the same constant external drive h_0. The sequence of rectangular activity pulses in the past therefore gives rise to an input potential

$$h(t) = h_0 + J_0 \int_0^{\infty} \varepsilon(s) A(t-s)\mathrm{d}s = h_0 + \sum_{k=0}^{\infty} J_0\,\varepsilon(t + kT) + \mathcal{O}\left[(\delta_k)^2\right], \tag{20.10}$$

which is identical for all neurons.

To determine the period T, we consider a neuron in the *center* of the square pulse which has fired its last spike at $\hat{t} = 0$. The next spike of this neuron must occur at $t = T$, i.e., in the center of the next square pulse. We use $\hat{t} = 0$ in the threshold condition for

https://doi.org/10.1017/CBO9781107447615.024 Published online by Cambridge University Press

spike firing, which yields

$$T = \min \left\{ t \,|\, \eta(t) + h_0 + J_0 \sum_{k=0}^{\infty} \varepsilon(t + kT) = \vartheta \right\} . \tag{20.11}$$

If a synchronized solution exists, (20.11) defines its period.

We now use the population equation of renewal theory, Eq. (14.5). In the limit of low noise, the interval distribution $P_I(t|\hat{t})$ becomes a δ-function: neurons that have fired at time $\hat{t}$ fire again at time $t = \hat{t} + T(\hat{t})$. Using the rules for calculation with δ-functions and the threshold condition (Eq. (20.11)) for firing, we find

$$A(t) = \left[1 + \frac{h'}{\eta'} \right] A(t - T_b), \tag{20.12}$$

where the prime denotes the temporal derivative. T_b is the "backward interval:" neurons that fire at time t have fired their previous spike at time $t - T_b$. According to our assumption $\eta' > 0$. A necessary condition for an increase of the activity from one cycle to the next is therefore that the derivative h' is positive – which is the essence of the locking theorem.

The locking theorem is applicable in a large population of SRM neurons (Gerstner *et al.*, 1996b). As discussed in Chapter 6, the framework of SRM encompasses many neuron models, in particular the leaky integrate-and-fire model. Note that the above locking argument is a "local" stability argument and requires that network firing is already close to the fully synchronized state. A related but *global* locking argument has been presented by Mirollo and Strogatz (1990).

20.2.2 Oscillations with irregular firing

In the previous subsection, we have studied fully connected homogeneous network models which exhibit oscillations of the neuronal activity. In the locked state, all neurons fire regularly and in near-perfect synchrony. However, experiments show that, though oscillations are a common phenomenon, spike trains of individual neurons are often highly irregular.

Periodic large-amplitude oscillations of the population activity are compatible with irregular spike trains if individual neurons fire at an average frequency that is significantly lower than the frequency of the population activity (Fig. 20.7). If the subgroup of neurons that is active during each activity burst changes from cycle to cycle, then the distribution of interspike intervals can be broad, despite a prominent oscillation. For example, in the inferior olivary nucleus, individual neurons have a low firing rate of one spike per second while the population activity oscillates at about 10 Hz. Strong oscillations with irregular spike trains have interesting implications for short-term memory and timing tasks (Kistler and De Zeeuw, 2002).

https://doi.org/10.1017/CBO9781107447615.024 Published online by Cambridge University Press

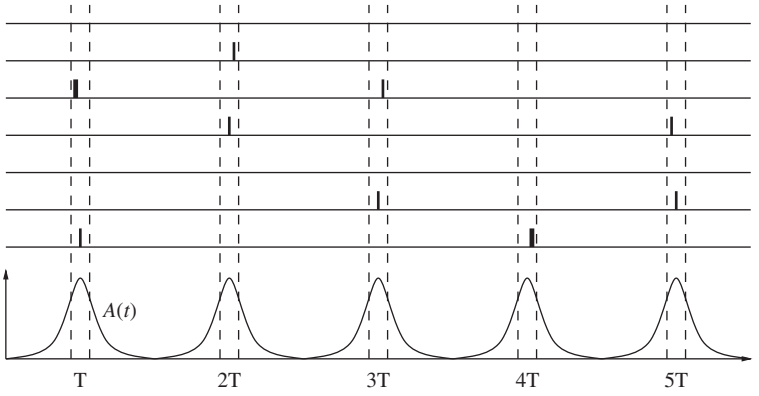

Fig. 20.7 Synchronous oscillation with irregular spike trains. Neurons tend to fire synchronously but with an average rate that is significantly lower than the oscillation frequency of the population activity (bottom). Each neuron is thus firing only in one out of approximately four cycles, giving rise to highly irregular spike trains. Short vertical lines indicate the spikes of a set of six neurons (schematic figure).

20.2.3 Phase models

For weak coupling, synchronization and locking of periodically firing neurons can be systematically analyzed in the framework of phase models (Kuramoto, 1984; Ermentrout and Kopell, 1984; Kopell, 1986; Pikovsky and Rosenblum, 2007).

Suppose a neuron driven by a constant input fires regularly with period T, i.e., it evolves on a periodic limit cycle. We have already seen in Chapter 4 that the position on the limit cycle can be represented by a phase ϕ. In contrast to Chapter 4, we adopt here the conventions that (i) spikes occur at phase $\phi = 0$ (Fig. 20.8) and (ii) between spikes the phase increases from zero to 1 at a constant speed $f_0 = 1$, where $f_0 = 1/T$ is the frequency of the periodic firing. In more formal terms, the phase of an uncoupled neural "oscillator" evolves according to the differential equation

$$\frac{\mathrm{d}}{\mathrm{d}t}\phi = f_0 \tag{20.13}$$

and we identify the value 1 with zero. Integration yields $\phi(t) = (t/T)_{\mathrm{mod1}}$ where "mod1" means "modulo 1." The phase ϕ represents the position on the limit cycle (Fig. 20.8a).

Phase models for networks of N interacting neurons are characterized by the intrinsic frequencies f_j of the neurons ($1 \le j \le N$) as well as the mutual coupling. For weak coupling, the interaction can be directly formulated for the phase variables ϕ_j,

$$\frac{\mathrm{d}}{\mathrm{d}t}\phi_i = f_i + \varepsilon \sum_j w_{ij} P(\phi_i, \phi_j), \tag{20.14}$$

where $\varepsilon \ll 1$ is the overall coupling strength, w_{ij} are the relative pairwise coupling, and P the phase coupling function. For pulse-coupled oscillators, an interaction from neuron j to

https://doi.org/10.1017/CBO9781107447615.024 Published online by Cambridge University Press

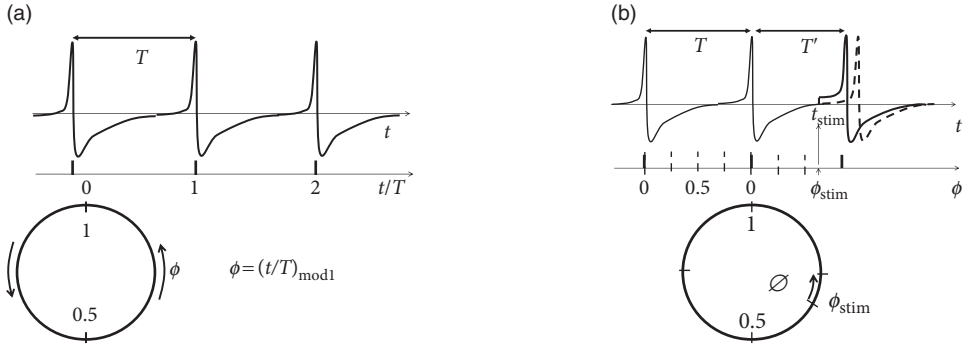

Fig. 20.8 Phase models. (a) For a neuron firing with period T (top), we can introduce a phase variable $\phi = (t/T)_{\mathrm{mod1}}$ (bottom). (b) If a weak input pulse of amplitude ε is given at a phase ϕ_{stim}, the interspike interval T' is shorter. The phase response curve $\tilde{F}(\phi_{\mathrm{stim}})$ measures the phase advance $\Delta\phi = (T - T')/T$ as a function of the stimulation phase ϕ_{stim}.

neuron i happens only at the moment when the presynaptic neuron j emits a spike. Hence the phase coupling function $P(\phi_i, \phi_j)$ is replaced by

$$P(\phi_i, \phi_j) \longrightarrow F(\phi_i) \sum_f \delta(t - t_j^f)\,, \tag{20.15}$$

where $\{t_j^1, t_j^2, t_j^3, \dots\}$ are the spike times of the presynaptic neuron, defined by the zero-crossings of ϕ_j, i.e., $\{t \,|\, \phi_j(t) = 0\}$. The function F is the "phase response curve": the effect of an input pulse depends on the momentary state (i.e., the phase ϕ_i) of the receiving neuron (see the below example below).

For neurons with synaptic currents of finite duration, phase coupling is not restricted to the moment of spike firing ($\phi_j = 0$) of the presynaptic neuron, but extends also to phase values $\phi_j > 0$. The phase coupling can be positive or negative. Positive values of P lead to a phase advance of the postsynaptic neuron. Phase models are widely used to study synchronization phenomena (Pikovsky and Rosenblum, 2007).

Example: Phase response curve

The idea of a phase response curve is illustrated in Fig. 20.8b. A short positive stimulating input pulse of amplitude ε perturbs the period of an oscillator from its reference value T to a new value T', which might be shorter or longer than T (Canavier, 2006; Winfree, 1980). The phase response curve $\tilde{F}(\phi_{\mathrm{stim}})$ measures the phase advance $\Delta\phi = (T - T')/T$ as a function of the phase ϕ_{stim} at which the stimulus was given.

Knowledge of the stimulation phase is, however, not sufficient to characterize the effect on the period, because a stimulus of amplitude 2ε is expected to cause a larger phase shift than a stimulus of amplitude 1ε. The mathematically relevant notion is there-

https://doi.org/10.1017/CBO9781107447615.024 Published online by Cambridge University Press

fore the phase advance, divided by the (small) amplitude ε of the stimulus. More precisely, the infinitesimal phase response curve is defined as

$$F(\phi_{\text{stim}}) = \lim_{\varepsilon \to 0} \frac{T - T'(\phi_{\text{stim}})}{\varepsilon T} . \tag{20.16}$$

The infinitesimal phase response curve can be extracted from experimental data (Gutkin *et al*., 2005) and plays an important role in the theory of weakly coupled oscillators.

Example: Kuramoto model

The Kuramoto model (Kuramoto, 1984; Acebron *et al*., 2005) describes a network of N phase oscillators with homogeneous all-to-all connections $w_{ij} = J_0/N$ and a sinusoidal phase coupling function

$$\frac{\mathrm{d}}{\mathrm{d}t}\phi_i = f_i + \frac{J_0}{N}\sum_{j=1}^{N} \sin(2\pi(\phi_j - \phi_i)), \tag{20.17}$$

where f_i is the intrinsic frequency of oscillator i. For the analysis of the system, it is usually assumed that both the coupling strength J_0 and the frequency spread $(f_i - \overline{f})/\overline{f}$ are small. Here $\overline{f}$ denotes the mean frequency.

If the spread of intrinsic frequencies is zero, then an arbitrary small coupling $J_0 > 0$ synchronizes all units at the same phase $\phi_i(t) = \phi(t) = \overline{f}\,t$. This is easy to see. First, synchronous dynamics $\phi_i(t) = \phi_j(t) = \phi(t)$ for all i, j are a solution of Eq. (20.17). Second, if one of the oscillators is late by a small amount, say oscillator n has a phase $\phi_n(t) < \phi(t)$, then the interaction with the others makes it speed up (if the phase difference is smaller than 0.5) or slow down (if the phase difference is larger than 0.5), until it is synchronized with the group of other neurons. More generally, for a fixed (small) spread of intrinsic frequencies, there is a minimal coupling strength J_c above which global synchronization sets in.

We note that, in contrast to pulse-coupled models, units in the Kuramoto model can interact at arbitrary phases.

20.2.4 Synaptic plasticity and oscillations

During an oscillation a large fraction of excitatory neurons fires near-synchronously (Fig. 20.4). What happens to the oscillation if the synaptic efficacies between excitatory neurons are not fixed but subject to spike-timing dependent plasticity (STDP)? In this subsection we sketch some of the theoretical arguments (Lubenov and Siapas, 2008; Pfister and Tass, 2010)

In Fig. 20.9 near synchronous spikes in a pair of pre- and postsynaptic neurons are shown together with a schematic STDP window; see Section 19.1.2. Note that the horizontal axis of the STDP window is the difference between the spike *arrival* time t^{pre} at the

https://doi.org/10.1017/CBO9781107447615.024 Published online by Cambridge University Press

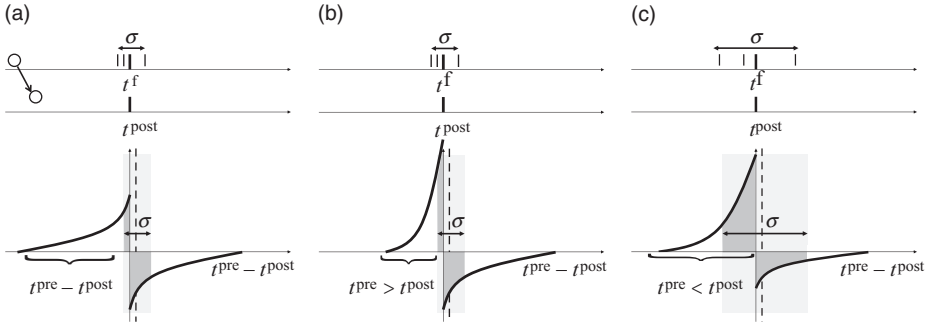

Fig. 20.9 Network oscillations and STDP. (a) Top: During a near-synchronous oscillation presynaptic spike timings t^f have a jitter σ with respect to the spike of a given postsynaptic neuron. Bottom: Because of axonal transmission delay, the spike *arrival* time $t^{\rm pre} = t^f + \Delta^{\rm ax}$ of presynaptic spikes at the synapse, is slightly shifted (light shaded area) to the regime "post-before-pre." Therefore, for an antisymmetric STDP window, synaptic depression dominates; compare the dark shaded areas for potentiation and depression. (b) Same as in (a), except that the amplitude of potentiation for near-synchronous firing is larger. As before, the total area under the STDP curve is balanced between potentiation and depression (the integral over the STDP curve vanishes). (c) Same as in (b), except that the integral over the STDP curve is now positive, as is likely to be the case at high firing rates. For large jitter σ potentiation dominates over depression (compare the dark-shaded areas).

presynaptic terminal and the spike firing time $t_i^f = t^{\rm post}$ of the postsynaptic neuron. This choice (where the presynaptic spike arrival time is identified with the onset of the EPSP) corresponds to one option, but other choices (Markram *et al.*, 1997; Sjöström *et al.*, 2001) are equally common. With our convention, the jump from potentiation to depression occurs if postsynaptic firing coincides with presynaptic spike arrival. However, because of axonal transmission delays, synchronous firing leads to spike arrival that is *delayed* with respect to the postsynaptic spike. Therefore, consistent with experiments (Sjöström *et al.*, 2001), synchronous spike firing with small jitter leads, at low repetition frequency, to a depression of synapses (Fig. 20.9a). Lateral connections within the population of excitatory neurons are therefore weakened (Lubenov and Siapas, 2008).

However, the shape of the STDP window is frequency dependent with a marked dominance of potentiation at high repetition frequencies (Sjöström *et al.*, 2001). Therefore, near-synchronous firing with a large jitter σ leads to a strengthening of excitatory connections (Fig. 20.9c) in the synchronously firing group (Pfister and Tass, 2010). In summary, synchronous firing and STDP tightly interact.

Example: Bistability of plastic networks

Since we are interested in the interaction of STDP with oscillations, we focus on a recurrent network driven by periodically modulated spike input (Fig. 20.10a). The

https://doi.org/10.1017/CBO9781107447615.024 Published online by Cambridge University Press

lateral connection weights w_{ij} from a presynaptic neuron j to a postsynaptic neuron i are changed according to Eq. (19.11), which we repeat here for convenience

$$\frac{\mathrm{d}}{\mathrm{d}t} w_{ij}(t) = S_j(t) \left[a_1^{\mathrm{pre}} + \int_0^\infty A_-(w_{ij}) W_-(s)\, S_i(t-s)\, \mathrm{d}s \right] + S_i(t) \left[a_1^{\mathrm{post}} + \int_0^\infty A_+(w_{ij}) W_+(s)\, S_j(t-s)\, \mathrm{d}s \right], \tag{20.18}$$

where $S_j = \sum_f \delta(t - t_j^f)$ and $S_i = \sum_f \delta(t - t_i^f)$ denote the spike trains of pre- and postsynaptic neurons, respectively. The time course of the STDP window is given by $W_\pm = \exp(-s/\tau_\pm)$ and a_1^{pre} and a_1^{post} are non-Hebbian contributions, i.e., an isolated presynaptic or postsynaptic spike causes a small weight change, even if it is not paired with activity of the partner neuron. Non-Hebbian terms $a_1^{\mathrm{pre}} + a_1^{\mathrm{post}} < 0$ are linked to "homeostatic" or "heterosynaptic" plasticity and are useful to balance weight growth caused by Hebbian terms (Chapter 19). The amplitude factors $A_\pm$ are given by soft-bounds analogous to Eq. 19.4:

$$A_+(w_{ij}) = A_+^0\, (w^{\max} - w_{ij})^\beta \quad \text{for } 0 < w < w^{\max}, \tag{20.19}$$

$$A_-(w_{ij}) = A_-^0\, (w_{ij})^\beta \quad \text{for } 0 < w < w^{\max}, \tag{20.20}$$

with $\beta = 0.05$. An exponent β close to zero implies that there is hardly any weight dependence except close to the bounds at zero and $w^{\max}$.

The analysis of the network dynamics in the presence of STDP (Pfister and Tass, 2010; Gilson *et al.*, 2009; Kempter *et al.*, 1999a) shows that the most relevant quantities are (i) the integral over the STDP window $A_+(w)\tau_+ + A_-(w)\tau_-$ evaluated at a value w far away from the bounds; (ii) the Fourier transform of the STDP window at the frequency $1/T$, where T is the period of the oscillatory drive; (iii) the sum of the non-Hebbian terms $a_1^{\mathrm{pre}} + a_1^{\mathrm{post}}$.

Oscillations of brain activity in the δ or θ frequency band are relatively slow compared to the time scale of STDP. If we restrict the analysis to oscillations with a period T that is long compared to the time scale $\tau_{+/-}$ of the learning window, the Fourier transform of the STDP window mentioned in (ii) can be approximated by the integral mentioned in (i). Note that slow sinusoidal oscillations correspond to a large jitter σ of spike times (Fig. 20.9c).

Pfister and Tass (2010) found that the network dynamics are bistable if the integral over the learning window is positive (which causes an increase of weights for uncorrelated Poisson firing), but weight increase is counterbalanced by weight decrease caused by homeostatic terms in the range $C < a_1^{\mathrm{pre}} + a_1^{\mathrm{post}} < c < 0$ with suitable negative constants C and c. Therefore, for the same periodic stimulation paradigm, the network can be in either a stable state where the average weight is close to zero, or a different stable state where the average weight is significantly positive (Fig. 20.10b). In the latter case, the oscillation amplitude in the network is enhanced (Fig. 20.10c).

https://doi.org/10.1017/CBO9781107447615.024 Published online by Cambridge University Press

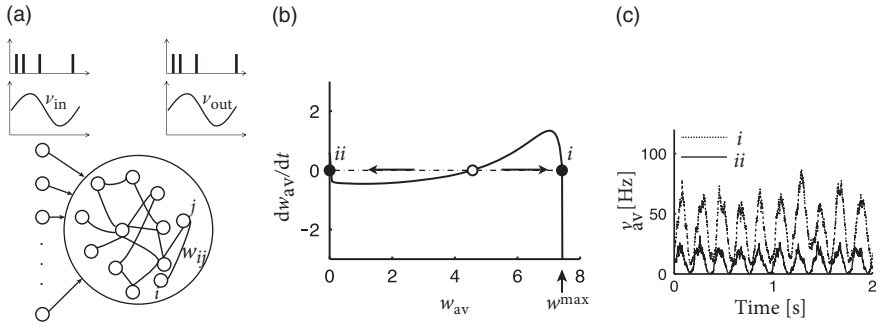

Fig. 20.10 Bistability of plastic networks. (a) A model network of spiking neurons receives spike input at a periodically modulated rate $\nu^{\rm in}$, causing a modulation of the firing rate $\nu_i^{\rm out}$ of network neurons $1 \le i \le N$. Lateral weights w_{ij} are subject to STDP. (b) Change $dw_{\rm av}/dt$ of the average weight as a function of $w_{\rm av}$. For an STDP window with positive integral the average network weight w_{av} exhibits bistability (arrows indicate direction of change) in the presence of the periodic input drive. The maximum weight is $w^{\rm max}$. (c) Bistability of the average network output rate $\nu_{\rm av} = (1/N)\sum_{i=1}^{N} \nu_i^{\rm out}$ in the presence of a periodic drive. The weights w_{ij} in the two simulations have an average value $w_{\rm av}$ given by the two fixed points in (b). Adapted from Pfister and Tass (2010).

20.3 Helping patients

We would like to close this chapter – and indeed the whole book – with an inspiring application of insights derived from the theory of neuronal dynamics to animals and, potentially, humans. Initial results at the current state of research are encouraging, so that mathematical considerations could ultimately increase the quality of life of, among others, Parkinsonian patients.

Parkinson's is a severe brain disease. A prominent symptom in human patients suffering from Parkinson's disease is involuntary shaking of arms and fingers in a periodic movement of about 3–6 Hz, called resting tremor. Some patients also exhibit muscle rigidity or akinesia where they are unable to move. Tremor as well as rigidity are correlated with overly strong oscillatory synchronization in brain areas such as thalamus and basal ganglia, whose activity in the healthy state is asynchronous (Pare *et al.*, 1990; Nini *et al.*, 1995; Tass *et al.*, 2010). Moreover, the oscillation frequency of neural activity is related to the tremor frequency.

One of the presently available treatments of Parkinsonian symptoms is "deep brain stimulation" (DBS) (Benabid *et al.*, 1991, 2009). DBS reduces both tremor and rigidity of Parkinsonian patients. To perform DBS, a high-frequency stimulus is applied to an electrode implanted in the subthalamic nucleus or globus pallidus (which project indirectly or directly onto the thalamus) of the patient (Fig. 20.11a). The treatment is reversible so that, when stimulation is stopped, patients rapidly fall back into tremor or rigidity.

If we view the brain as a dynamical system, we can say that classical DBS shifts the state of the brain so as to reduce the symptoms of Parkinson's during stimulation, but does not return the brain's autonomous dynamics back to a healthy state. In other words, the

https://doi.org/10.1017/CBO9781107447615.024 Published online by Cambridge University Press

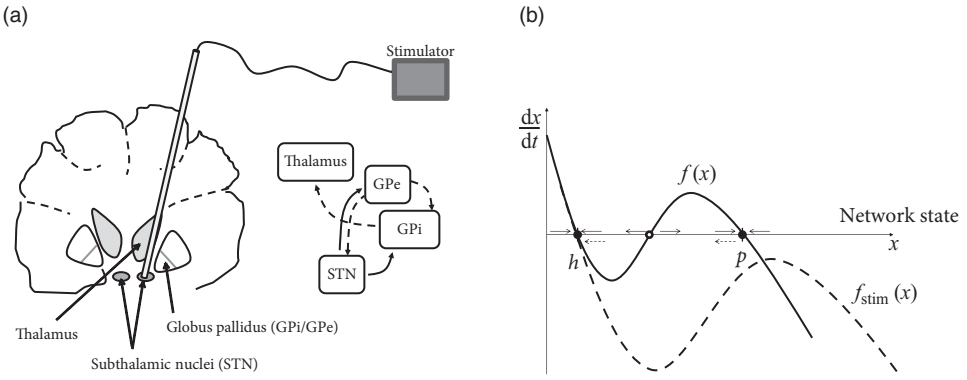

Fig. 20.11 Deep brain stimulation. (a) Schema showing a vertical cut through the brain with implanted electrode. The tip of the electrode reaches one of the subthalamic nuclei. The electrode is connected with a wire to the stimulator. The box diagram shows some of the major excitatory (solid arrows) and inhibitory (dashed arrows) connections from the subthalamic nucleus (STN) to thalamus. (b) Bistability of a healthy (h) and pathological network state (p, circle), described by the flow (solid arrows) of an abstract differential equation $\mathrm{d}x/\mathrm{d}t = f(x)$ (solid line). To kick the network out of the pathological state, an appropriate stimulus has to be applied that destabilizes p and drives the network state toward h by changing the right-hand side of the differential equation to $f_{\mathrm{stim}}(x)$ (dashed line and arrows); adapted from Pfister and Tass (2010).

patient relies on continuous treatment through DBS. We may visualize the pathological and healthy conditions as two different configuration in some abstract space of network states. It is reasonable to assume that brain dynamics in the healthy state is at a stable equilibrium point – despite ongoing spike firing and plasticity on different time scales; otherwise our brains would rapidly stop functioning. The fact that, after the end of DBS, the brain returns to the pathological state indicates that this state is also stable (Fig. 20.11b).

The question arises whether, by suitable stimulation protocols, it would be possible to shift the pathological brain back into its healthy state. Work of the group of Peter Tass (Tass, 2003; Tass *et al*., 2012b), but also other groups (Rubin and Terman, 2004; Rosin *et al*., 2011; Wilson *et al*., 2011) suggests that this may be possible. The treatment relies on the idea that the pathological state of strong oscillations is probably linked to pathologically strong intranetwork connections (Fig. 20.10c). An ideal stimulation protocol should thus not only interfere with the oscillations but also lead to a rewiring of the network with weaker connections so that, even when the stimulus is removed, the network does not immediately fall back into the strong oscillatory mode.

How can we interfere with an ongoing synchronized oscillation? As discussed in Section 20.2, neurons in an oscillatory state can be described by a phase ϕ. An electric pulse delivered by an electrode tends to synchronize neurons in the neighborhood of the electrode by shifting their phases by an amount that depends on the current phase of the neuron. If several electrode fibers are used in the same network, local groups surrounding the tips of the fibers can be stimulated at different moments in time. Therefore, the phase within each

https://doi.org/10.1017/CBO9781107447615.024 Published online by Cambridge University Press

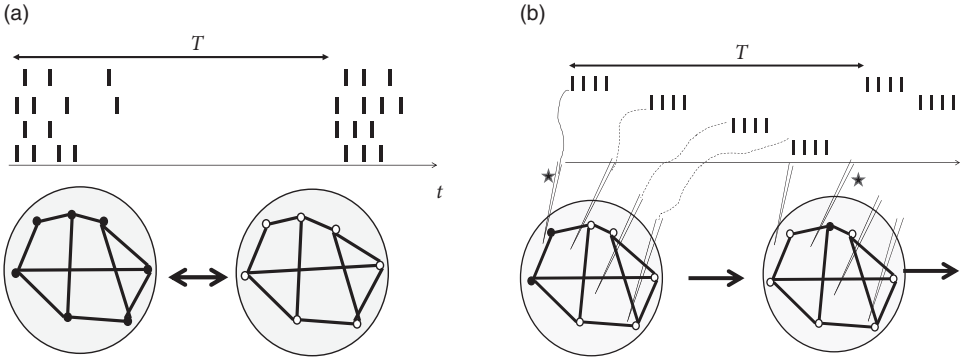

Fig. 20.12 Coordinated reset stimulation. (a) A population of neurons exhibits synchronous firing activity with period T (schematic). (b) If subgroups of neurons are stimulated at intervals $T/4$, the synchronous oscillation is interrupted ("coordinated reset" of oscillators). The stimulation can be delivered directly in the population or in one of the nuclei projecting onto it. Schematic, after Tass (2003).

group is reset by roughly the same amount, but the phase shift varies between groups. Consider a stimulation of four fibers given at a relative interval of $T/4$ (Fig. 20.12). With such a stimulation paradigm, the global network synchronization is perturbed by the "coordinated reset" of the four subpopulations (Tass, 2003). With eight or twenty independent electrode fibers one could spread out the stimulation (and therefore the phases of neuronal oscillators) even more equally over one period. However, the number four is a reasonable compromise and bundles of four fibers attached together so as to form one single electrode device are readily available.

If a single sequence of four "coordinated reset" pulses is given to four electrode fibers, the network returns, after some transients, to the synchronized oscillation. In order to make the asynchronous state stable, the network wiring needs to be changed. Hebbian synaptic plasticity requires neurons to be active. It is therefore important to choose a stimulation protocol which suppresses synchronous oscillations, but not neuronal activity *per se*. The "coordinated reset" fulfills this condition since it does not silence the neural oscillators but just shifts their phases. Therefore, if the "coordinated reset" stimulation is repeated again and again, so as to keep network activity in a state of asynchronous firing for a sufficiently long time, we may expect that synaptic plasticity causes a rewiring of the network connectivity. Once the network is rewired, the stimulus can be removed.

Indeed, when monkeys suffering from Parkinsonian symptoms have received a few hours of DBS with the "coordinated reset" protocol, symptoms are reduced and remain at a reduced level for more than 24 hours (Fig. 20.13b), before they slowly drift back into the oscillatory state (Tass *et al.*, 2012b). The beneficial effects of "coordinated reset" stimulation therefore last at least 10 times longer than those of traditional DBS where tremor reappears rapidly.

From the perspective of dynamical systems, these results suggest that the healthy state of Parkinsonian patients is not globally stable. However, since the "ruins" (see Chapter 4)

https://doi.org/10.1017/CBO9781107447615.024 Published online by Cambridge University Press

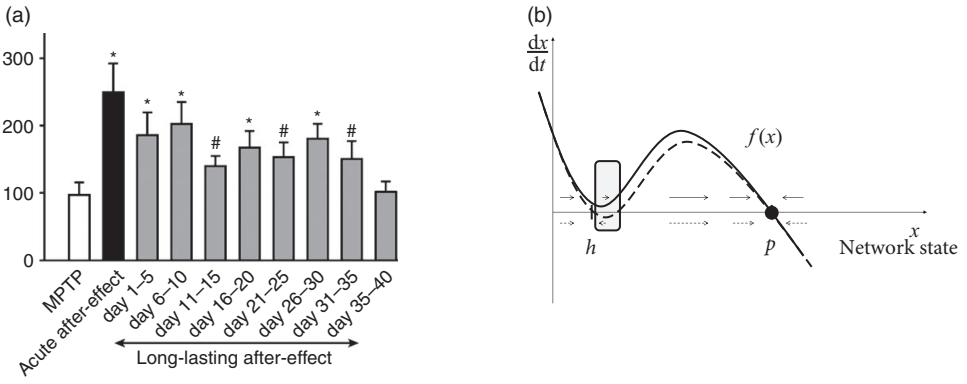

Fig. 20.13 Long-lasting plasticity effects. (a) Behavioral performance (vertical) of monkeys suffering from Parkinsonian symptoms before ("MPTP") and after treatment with coordinated reset stimulation. Stimulation led to an improvement of behavior that persisted for many days after the end of stimulation. From Tass *et al*. (2012b) with permission from IOS Press. (b) Dynamical systems interpretation: In contrast to Fig. 20.11b, the healthy state h of MPTP monkeys is either not a fixed point at all (solid line) or a marginally stable one (dashed line), but in both cases the flow in the vicinity of the healthy state (gray area) is slowed down, so that the return to the pathological state takes some time.

of the fixed point corresponding to healthy asynchronous activity persist, a shift of the network into the neighborhood of the healthy state leads to a slow down of the dynamics so that the network remains for a long time in the neighborhood of the healthy condition (Fig. 20.13c).

Traditional protocols of DBS have been found by trial and error. The standard protocol consists of continuous high-frequency stimulation (>100 Hz) at rather large amplitude (Benabid *et al*., 1991). Remarkably, the mathematical perspective provided by the theory of dynamical systems together with intensive computational modeling (Tass, 2003; Rubin and Terman, 2004; Wilson *et al*., 2011; Pfister and Tass, 2010) has now led to protocols that work with reduced amplitude and do not require continuous stimulation. Instead, only a few hours of stimulation per day promise to suffice (Tass *et al*., 2012b). Eventually, we may hope that these or related (Rosin *et al*., 2011) protocols will be translated from monkeys to humans and increase the quality of life of patients suffering from severe forms of Parkinson's disease. Interestingly, the "coordinated reset" protocol has already found a first successful application in humans suffering from tinnitus (Tass *et al*., 2012a).

20.4 Summary

Reservoir computing uses the rich dynamics of randomly connected networks as a representation on which online computation can be performed. Inhibitory synaptic plasticity may tune networks into a state of detailed balance where strong excitation is counterbal-

anced by strong inhibition. The resulting network patterns exhibit similarities with cortical data.

Oscillations are present in multiple brain areas, and at various frequencies. Oscillations in networks of coupled model neurons can be mathematically characterized as an instability of the stationary state of irregular firing (see Chapters 13 and 14) or as a stable limit cycle where all neurons fire in synchrony. The stability of perfectly synchronized oscillation is clarified by the locking theorem: a synchronous oscillation is stable if the spikes are triggered during the rising phase of the input potential, which is the summed contribution of all presynaptic neurons. Stable synchronous oscillations can occur for a wide range of parameters and for both excitatory and inhibitory couplings.

Phase models describe neurons in the oscillatory state. If a stimulus is given while the neuron is at a certain phase, its phase shifts by an amount predicted by the phase response curves and the size of the stimulus.

Oscillatory activity has been linked to numerous brain diseases, in particular Parkinson's. Modern protocols of DBS aim at exploiting the interaction between phase response curves, oscillations, and synaptic plasticity so as to reduce the motor symptoms of Parkinson's disease.

Literature

The potential computational use of the rich network dynamics of randomly connected networks has been emphasized in the framework of "liquid computing" (Maass *et al*., 2002) and "echo state networks" (Jaeger and Haas, 2004). The network dynamics can be influenced by a variety of optimization algorithms (Jaeger and Haas, 2004; Maass *et al*., 2007; Sussillo and Abbott, 2009; Hoerzer *et al*., 2012) and the resulting networks can be analyzed with principles from dynamical systems (Ganguli *et al*., 2008; Sussillo and Barak, 2013). The theory of random neural networks has been developed around the eigenvalue spectrum of connectivity matrices (Rajan and Abbott, 2006) and the notion of chaos (Sompolinksy *et al*., 1988).

Synchronization is a traditional topic of applied mathematics (Winfree, 1980; Kuramoto, 1984). For pulse-coupled units, synchronization phenomena in pulse-coupled units have been widely studied in a non-neuronal context, such as the synchronous flashing of tropical fireflies (Buck and Buck, 1976), which triggered a whole series of theoretical papers on synchronization of pulse-coupled oscillators (see, e.g., Mirollo and Strogatz, 1990). The locking theorem (Gerstner *et al*., 1996b) is formulated for SRM neurons which cover a large class of neuronal firing patterns and includes the leaky integrate-and-fire model as a special case (see Chapter 6). The more traditional mathematical theories are typically formulated in the phase picture (Winfree, 1980; Kuramoto, 1984; Pikovsky and Rosenblum, 2007) and have found ample applications in the mathematical neurosciences (Gutkin *et al*., 2005; Canavier, 2006).

Oscillations in the visual system and the role of synchrony for feature binding have been reviewed by Singer (1993, 2007). Oscillations in sensory systems have been reviewed

by Ritz and Sejnowski (1997) and, specifically in the context of the olfactory system, by Laurent (1996), and the hippocampus by O'Keefe and Recce (1993) and Buzsaki (2011). For oscillations in EEG, see Bazhenov and Timofeev (2006).

The classic work on DBS is Benabid *et al*. (1991). The interplay between mathematical theories of neuronal dynamics and DBS is highlighted in the papers of Rubin and Terman (2004), Wilson *et al*. (2011), Pfister and Tass (2010), and Tass (2003).